

# STUDY ON CREEP CHARACTERISTICS OF SALT ROCK UNDER UNLOADING CONDITIONS

Bo Chen<sup>1</sup>, \*Zongze Li<sup>1</sup>, Chun Liu<sup>2</sup>, Chao Du<sup>3</sup>, Deyi Jiang<sup>1</sup>

<sup>1</sup>State Key Laboratory for the Coal Mine Disaster Dynamics and Controls, Chongqing University, China;

<sup>2</sup>Safety Engineering College, Chongqing University of Science and Technology, China

<sup>3</sup>China Southwest Geotechnical Investigation & Design Institute Co., Ltd., China

\*Corresponding Author; Received:08 March 2020, Revised:12 Sept.2020, Accepted:26 Dec.2020

**ABSTRACT:** The underground salt karst caverns are considered as an excellent oil and gas reserve site due to the dense low permeability and excellent creep. The creep characteristics of salt rocks under frequent gas injection and gas production activities are the focus of salt cavern gas storage. The 700h loading and unloading creep tests were performed on salt samples taken from Jintan, Jiangsu Province, China, and the creep behaviors of rock salt under different loading and unloading stress paths were compared and analyzed. The results showed that the steady-state creep strain rate increases with the increase of deviatoric stress during multi-stage creep test, The deviatoric stress has a great influence on the steady-state creep strain rate, and the steady-state creep strain rate increases obviously with the increase of the deviator stress in the loading stage, but in the unloading stage, steady-state creep strain rate increases with deviatoric stress increase, and the increase range is small. The Fractional Derivative model, the Nishihara model and the Burgers model are used to fit the experimental data of the initial creep stage and the steady-state creep stage during loading stage, the results show that the Fractional Derivative model can better describe the creep curve. The creep deformation curve is almost straight and the creep curve is fitted by a linear function in unloading stage, the results show that the fitting curve is consistent with the experimental results.

*Key words: Salt rock, Loading and unloading, Creep, Creep model*

## 1. INTRODUCTION

Salt rock, as an ideal medium for energy storage and permanent disposal of high-radioactive nuclear waste, has excellent creep properties, low permeability and good self-healing features when damaged [1-6]. Underground cavities leached in salt rock have been used proverbially for storing energy (Such as natural gas [7], oil and compressed air/hydrogen [8]) in North America and Asia [9,10]. Nuclear waste remains radioactive over millions of years, so underground cavities in salt rock have been used to store nuclear waste in Germany HerfaNeurode and Morsleben mines [11], and in the USA at the Waste Isolation Pilot Plant [12]. The stability of the storage cavity construction period and long-term operation period is extremely important when salt rock as a medium for underground energy storage [13-15]. The volume loss of the storage cavity is unavoidable in the long-term operation of salt rock storage, and the creep of the salt rock will deform the storage and reduce the volume convergence. It is necessary to control the volume shrinkage of the storage cavity within a certain range in order to ensure the normal operation of the energy

storage. The volume of the cavity is changing constantly due to the cavity is constantly pressurized and depressurized during the long-term operation of salt rock storage. Controlling the volume of the cavity is the key to ensure the stability of the reservoir, therefore, it's important to study the creep characteristics of salt rock.

Many research results show that the deformation characteristics and strength characteristics of salt rock [16-20]. Several studies have shown that the creep behavior of rock salt is dependent on factors such as the loading stress [21], loading type [22,23], loading rate [24], crystal size and contact between crystals [25], time [26], temperature [27], loading history [20]. Frequent gas injection and gas recovery activities keep the salt rock cavity under constant pressure and pressure relief state in the operation of salt rock gas storage, which is the research focus of creep characteristics. The creep characteristics of salt rock under different stress levels are that the creep deformation and creep rate increase as the stress level increases [28]. Many scholars have studied the salt rock grading loading test, which show long-term strength of salt rock [29], strain-hardening behavior of salt rock [30] and the creep model of salt rock [22].

The continuous cyclic loading tests and discontinuous cyclic loading tests of salt rock show that the fatigue life is dependent on amplitude and stress [31], frequency [32], loading rate [33], the number of cycles [34], and interval time [35,36]. Several scholars However, many tests are under monotonic increase in stress or cyclic loading and unloading, which doesn't better describe the continuous loading and unloading process of the gas storage during operation. Therefore, it is of great significance to study the creep characteristics of salt rocks under complex stress paths.

Despite a large number of studies show that the creep characteristics of salt rock under different paths, the creep characteristics of salt rocks under complex stress paths is not well documented. In this paper, multi-stage loading and unloading creep tests were performed on salt samples taken from Jintan, Jiangsu Province, China. The purpose of creep tests is to analyze the creep deformation characteristics of salt rock under constant confining and axial pressure increase, and to analyze the creep deformation characteristics and differences of salt rock under two loading histories. The Fractional Derivative model, Nishihara model and Burgers model are used to fit the test data in the initial creep stage and steady-state creep stage, and the linear equation is used to fit the test data in the unloading stage. The creep test of salt rock can provide theoretical reference for the long-term stability study of salt cavern gas storage.

## 2. MATERIAL AND METHODS

### 2.1 Experiment Setup and Specimens

The creep test was performed by using RC-2000 rock servo triaxial rheological testing machine of Wuhan Institute of Rock and Soil Mechanics, Chinese Academy of Sciences.



Fig.1: Manufactured salt samples

The salt rock samples are taken from the Jintan Salt Mine, Jiangsu Province, China, and were drilled from a buried depth of 720 ~ 1035 m, mainly containing sodium chloride, but also containing some other uniform impurities, showing a gray black.

According to rock mechanics test standards, all samples are processed into standard 50 mm×100 mm cylinders and the processed specimens are shown in Fig.1.

Fig.2 shows an electron micrograph of pure salt rock. As illustrated in this figure, the salt rock grain crystals are colorless. Block crystals can be clearly seen on the surface of some samples, and the block crystal contains small grains with regular shape and hexahedron. It can be seen from the microstructure that the surface of pure salt rock is extremely flat, smooth and dense, with no pores visible on the surface, indicating good tightness.

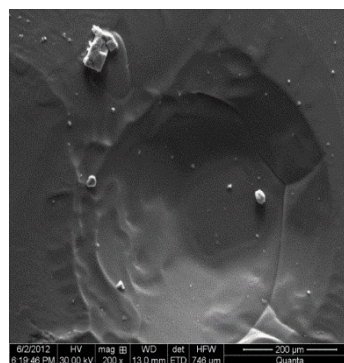


Fig.2: Colorless transparent rock salt under Scanning Electron Microscopy

### 2.2 Test Procedure

This paper carried out a creep test of constant confining pressure and axial multi-stage loading and unloading. The constant confining pressure is 5MPa, and the axial pressure is 20MPa, 25MPa, 30MPa, 35MPa. Figure 3 shows that stress state of the multi-stage loading and unloading creep test. Fig.3 shows the test steps:

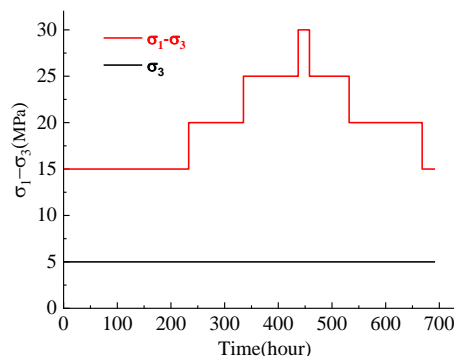


Fig.3: Stress state of the multi-stage loading and unloading creep test

- (1)The confining pressure adding rate is 0.1MPa/s until to 5MPa;
- (2) Keeping the confining pressure constant, the axial pressure adding rate is 0.1MPa/s until to 20MPa

and keep the axial pressure constant (the deviatoric stress is 15MPa);

(3) After entering the steady-state creep stage in (2), tests with axial pressures of 25MPa, 30MPa, and 35MPa will be performed respectively;

(4) Keeping the confining pressure constant and reduce the axial pressure from 35MPa to 30MPa at a rate of 0.1MPa/s (the deviatoric stress is 25MPa);

(5) After entering the steady-state creep stage in (2), tests with axial pressures of 25MPa and 20MPa will be performed respectively.

### 3. RESULTS AND ANALYSIS

#### 3.1 Deformation Characteristics

The stress-strain curve with confining pressure of 5MPa as shown in Fig.4. The triaxial compressive strength of salt rock is 64.6MPa, and a more obvious plastic zone, showing a transition state from brittleness

to plastic transformation.

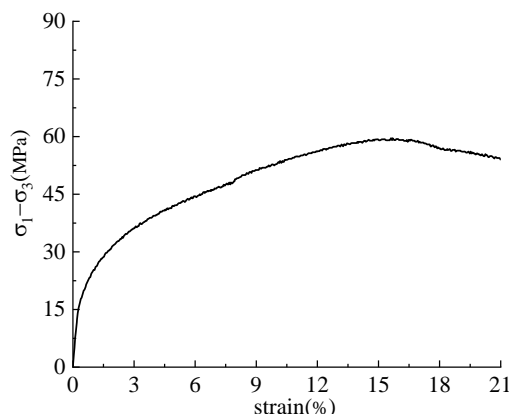


Fig.4: Stress-strain curve of rock salt under the confining pressures 5 MPa

Table1: Detailed deformation characteristics of rock salt under multi-stage creep test

Parameter State	Deviatoric stress(MPa)	Time (hour)	Steady-state creep strain rate(s <sup>-1</sup> )
Loading stage	15	232	2.15 × 10 <sup>-7</sup>
	20	105	1.18 × 10 <sup>-6</sup>
	25	105	2.42 × 10 <sup>-6</sup>
	30	21	1.12 × 10 <sup>-5</sup>
Unloading stage	25	73	2.95 × 10 <sup>-7</sup>
	20	137	6.17 × 10 <sup>-8</sup>
	15	24	0

The multi-stage creep tests were performed under constant confining pressure and axial pressure loading and unloading, which contains four stages of loading and four stages of unloading. Fig.5 shows the creep curve of multi-stage loading and unloading creep test. The detailed deformation characteristics of rock salt in the multi-stage creep tests are shown in Table 1.

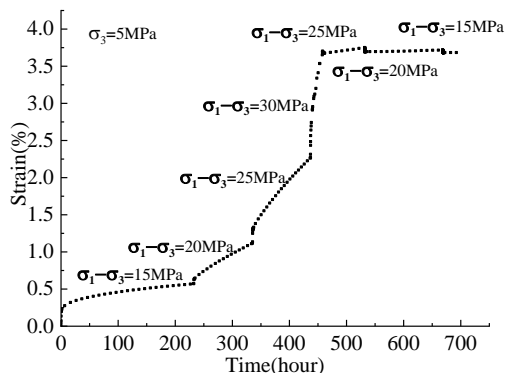


Fig.5: Creep curve of multi-stage loading and unloading creep test

Fig.6 shows the creep curve of multi-stage loading

creep test when deviatoric stress is progressively loaded from 15MPa to 30MPa with confining pressure of 5MPa, and the deviatoric stress increases by 5MPa per stage.

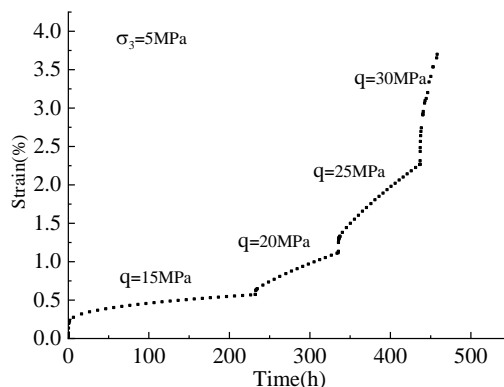


Fig.6: Creep curve of multi-stage loading creep test

This steady-state creep strain rate is 2.157E-7/s, 11.773E-7/s, 24.186E-7/s and 111.773E-7/s under the deviatoric stress of 15MPa, 20MPa, 25MPa and 30MPa, respectively. The specimen undergoes instantaneous deformation with each increase in axial

stress, after the instantaneous deformation, the specimen passes through a short initial creep stage and then enters the steady-state creep stage. This strain is 0.573%、0.543%、1.151% and 1.433% under the deviatoric stress of 15MPa, 20MPa, 25MPa and 30MPa, respectively. It shows that the deviatoric stress level has an enhancing effect on the amount of axial creep strain of the salt during the initial creep stage and steady-state creep stage.

Fig.7 shows the creep curve of multi-stage loading creep test when deviatoric stress is progressively unloaded from 30MPa to 15MPa with confining pressure of 5MPa, and the deviatoric stress decreases by 5MPa per stage.

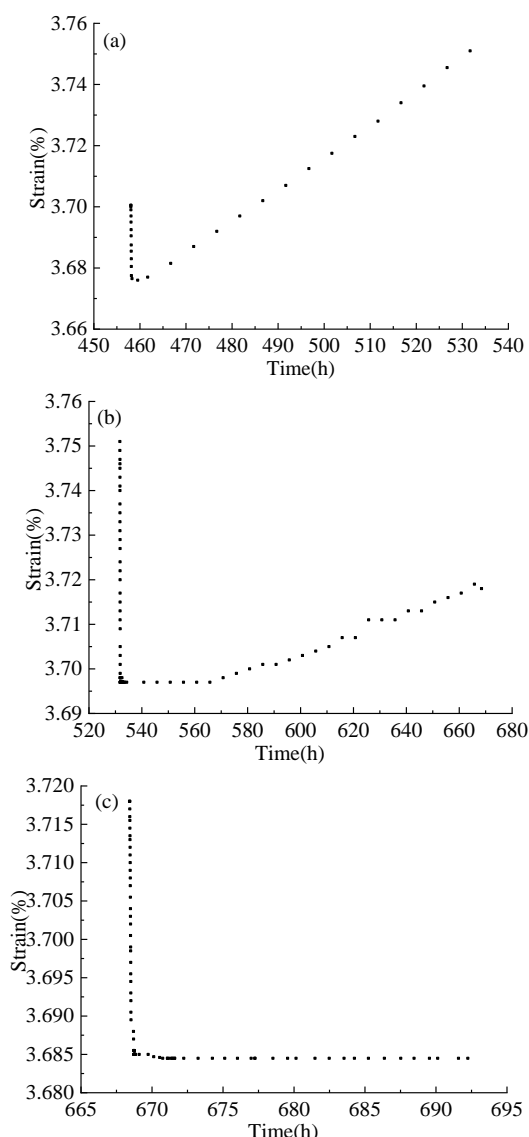


Fig.7: Creep curve of unloading stage (a)  $\sigma_1=30\text{MPa}$  and  $\sigma_3=5\text{MPa}$ , (b)  $\sigma_1=25\text{MPa}$  and  $\sigma_3=5\text{MPa}$ , (c)  $\sigma_1=20\text{MPa}$  and  $\sigma_3=5\text{MPa}$ .

As can be seen from Fig. 7, after each unloading, the specimen has an instantaneous elastic strain

recovery. The instantaneous elastic strain is 0.024%、0.054% and 0.033% under the deviatoric stress of 25MPa, 20MPa and 15MPa, respectively. After each unloading of the axial stress, the test directly enters the steady-state creep stage when a period of static state is finished, without the initial creep stage, which is obviously different from the loading stage. This steady-state creep strain rate is  $2.951\text{E-}7/\text{s}$ ,  $6.17\text{E-}8/\text{s}$  and 0 under the deviatoric stress of 25MPa, 20MPa and 15MPa, respectively.

### 3.2 Characteristics of Steady-state Creep Strain Rate

The relationship between deviatoric stress and steady-state creep strain rate in the creep test as shown in Fig.8, which contains deviatoric stress progressively loaded from 15 MPa to 30 MPa and deviatoric stress progressively unloaded from 30 MPa to 15 MPa with confining pressure of 5 MPa. The steady-state creep strain rate increases with the increase of deviatoric stress in the whole test. However, during the loading stage, deviatoric stress has a great influence on the steady-state creep strain rate, and the steady-state creep strain rate increases obviously when deviatoric stress increases, and during the unloading stage, although the steady-state creep strain rate increases with the increase of deviatoric stress, the increase range is small.

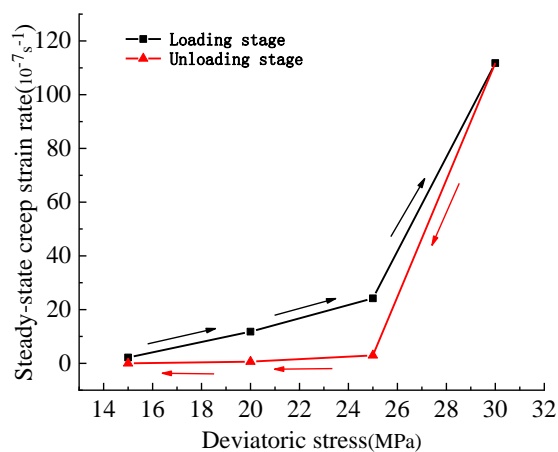


Fig.8: Steady-state creep strain rate versus deviatoric stress

## 4. ANALYSIS OF CREEP MODEL

### 4.1 Creep Model of Loading Stage

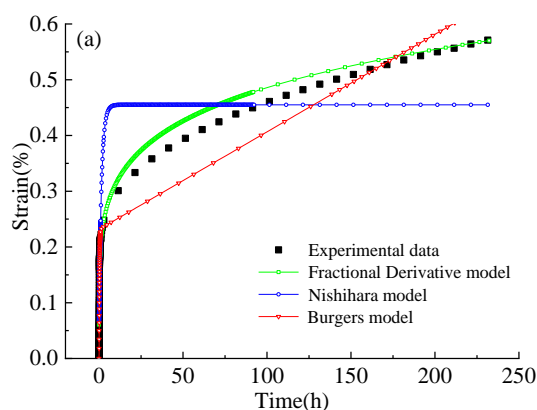
The deformation of the rock in the conventional creep test shows three stages: the initial creep stage, the steady-state creep stage, and the accelerating creep stage, which are mainly related to the expansion and evolution of fractures and pores in rocks. In general, the rock is in a natural state without pressure before

loading, and some of the pore fissures are in an open state. During the loading process, in the initial creep stage, the cracks in the rock are in an open state but do not expand; in the steady-state creep stage, existing cracks in the rock expand and are accompanied by the generation and expansion of new cracks; in the accelerated creep stage, the growth rate of cracks is accelerated, and the unstable expansion of cracks leads to rock failure [37].

The creep test of salt rock shows the normal initial creep stage and steady-state creep stage. The Fractional Derivative model, Nishihara model, and Burgers model were used to fit and analyze the experimental data in the initial creep stage and the steady-state creep stage. Since only initial creep stage and steady-state creep stage are considered, so  $\sigma < \sigma_s$ .

When  $\sigma < \sigma_s$ , the constitutive relationship of the Fractional Derivative creep model is simulated by the following equation [38].

$$\varepsilon(t) = \frac{\sigma}{E_1} + \frac{\sigma}{\eta_1} \frac{t^\beta}{\Gamma(\beta+1)} \quad (1)$$



When  $\sigma < \sigma_s$ , the constitutive relationship of the Nishihara model is simulated by the following equation [39].

$$\varepsilon(t) = \frac{\sigma}{E_1} + \frac{\sigma}{E_2} \left[ 1 - \exp\left(\frac{-E_2}{\eta_1} t\right) \right] \quad (2)$$

When  $\sigma < \sigma_s$ , the constitutive relationship of the Burgers model is simulated by the following equation [40].

$$\varepsilon(t) = \frac{\sigma}{E_1} + \frac{\sigma}{\eta_1} t + \frac{\sigma}{E_2} \left[ 1 - \exp\left(\frac{-E_2}{\eta_2} t\right) \right] \quad (3)$$

Where  $E_1, E_2$  and  $\eta_1, \eta_2$  are the elastic parameters and viscous parameters of each model.

By using the Fractional Derivative model, Nishihara model and Burgers model, the creep test data were fitted and analyzed by the self-defined function fitting tool of Origin numerical analysis software. The fitting results are shown in Fig.9.

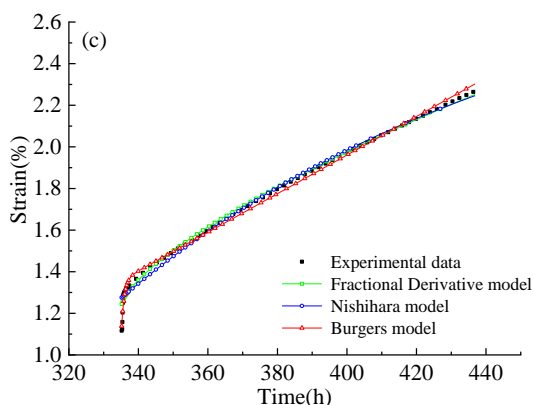
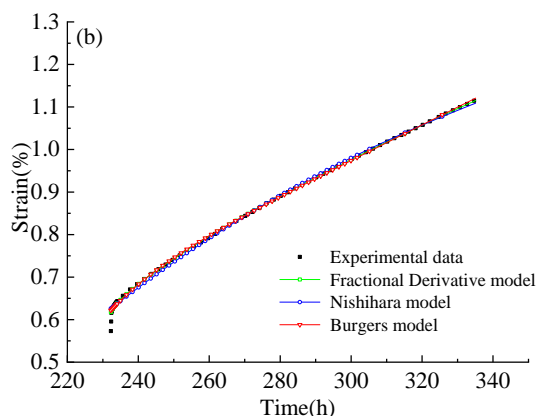


Fig.9 Comparison fitting curves and test data at loading stage: (a) deviatoric stress of 15MPa, (b) deviatoric stress of 20MPa, (c) deviatoric stress of 25MP

In Fig.9, the Fractional Derivative model of the three creep models can better describe the creep curve with deviatoric stress of 15 MPa, all three models can describe the creep curve well with deviatoric stress of 20MPa and 25MPa, so the Fractional Derivative

model can better describe the creep curve during loading than the other two models. The fitting parameters obtained by Fractional Derivative model fitting are shown in Table 2.

Table2: Fractional Derivative creep model parameters

Parameters	Deviatoric stress /MPa		
	15	20	25
$E_1 / GPa$	$3.7 \times 10^{14}$	0.447	0.195
$\eta_1 / GPa \cdot h^\beta$	0.08	1.63	0.727
$\beta$	0.19	0.783	0.710

During the long-term operation of salt cavern gas storage, the surrounding rocks are in a long-term steady-state creep stage. It is of great significance to study the relationship between steady-state creep strain rate and deviatoric stress, the relationship between deviatoric stress and steady-state creep strain rate can be expressed by exponential function [41]. The exponential function is used to fit and analyze the experimental data in the loading stage. The fitting result is shown in Fig.10, the correlation coefficient reaches 0.995, and the fitting function in the loading stage is simulated by the following equation.

$$\dot{\epsilon} = 0.022 \exp(0.285\sigma) \tag{4}$$

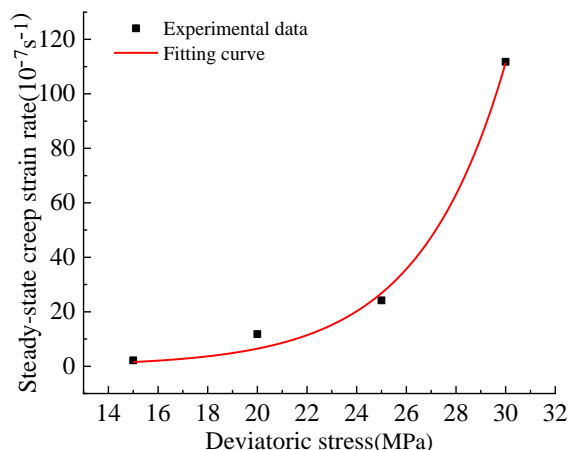


Fig.10: Fitting curve of steady-state creep strain rate and deviatoric stress at loading stage

### 4.2 Creep Model of Unloading Stage

During unloading stage, the deformation of the salt rock has only the steady-state creep stage, without the initial creep stage, which is due to the pore fissures in the rock salt have been compacted. In practical engineering, the change of surrounding rock stress

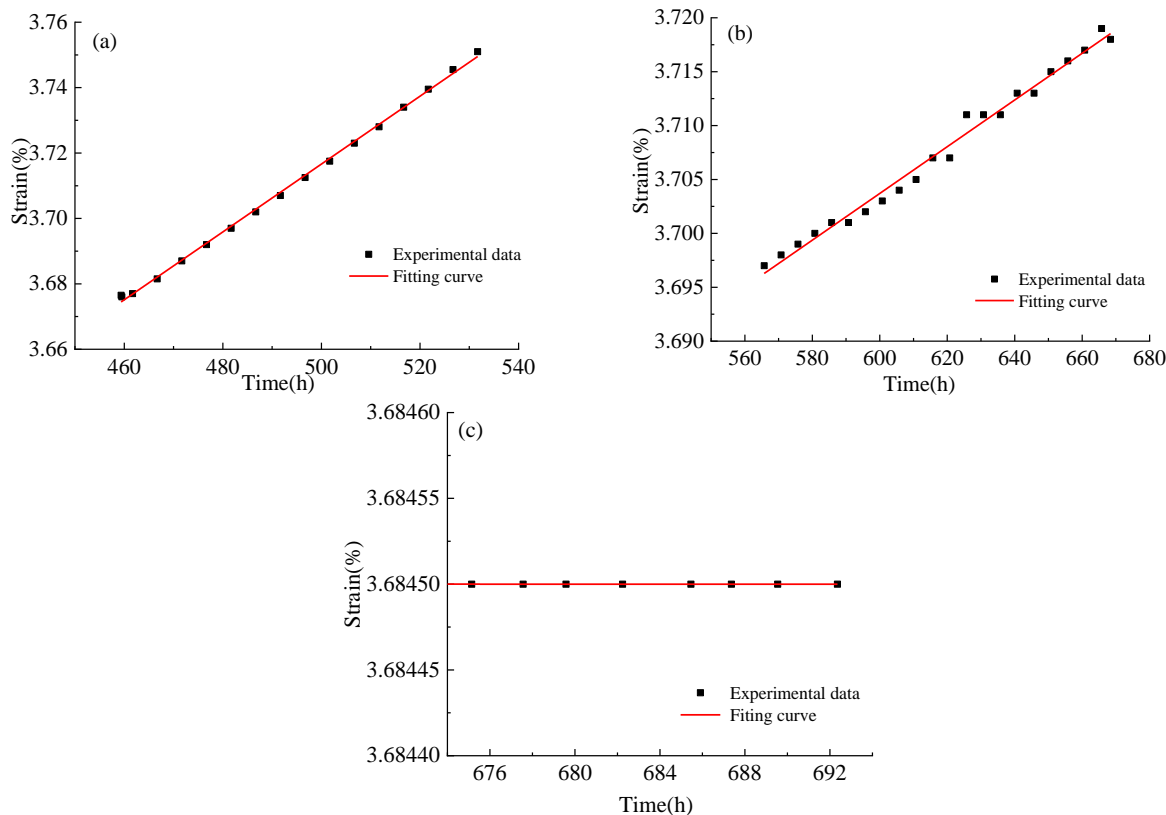


Fig.11: Comparison fitting curves and test data at unloading stage: (a) deviatoric stress of 25MPa, (b) deviatoric stress of 20MPa, (c) deviatoric stress of 15MPa

state is mostly a unloading process, which is one of the

reasons why in most numerical analyses of salt cavern

gas storage, only the deformation of rock salt in the steady-state creep stage is considered, while the initial creep is ignored. However, even under the same stress conditions, the steady-state creep strain rates of the loading and unloading stages show a large difference. Therefore, studying the creep deformation rate at the unloading stage is more significant for salt cavern gas storage.

From Fig.7, it can be concluded that during the unloading stage, rock salt of each stress level directly enters the steady-state creep stage, without the initial creep stage, and the deformation curve is almost straight. Therefore, a univariate linear function is used to fit the creep curve during the unloading stage. The fitting function in the unloading stage is simulated by the following equation.

$$\varepsilon = At + b \tag{5}$$

Where A is steady-state creep strain rate and b is a time-dependent parameter.

Linear functions are used to fit the test data in unloading stage, and the creep test data are fitted and identified with the custom function fitting tool of Origin numerical analysis software. The fitting results are shown in Fig.11, and the fitting parameters are shown in Table3.

Table3: Creep model parameters

Parameters	Deviatoric stress /MPa		
	25	20	15
A/s <sup>-1</sup>	2.80x10 <sup>-7</sup>	6.02x10 <sup>-8</sup>	0
b	3.199	3.573	3.6845

In Fig.11, when deviatoric stress are 25MPa, 20MPa and 15MPa, the fitting curve and the creep deformation curve have a high degree of coincidence, and the fitting correlation coefficients have reached 0.99, therefore, the linear function can simulate the creep curve during the unloading stage. Table 3 shows that the steady-state creep strain rate is 2.80e-7/s, 6.02e-8/s and 0 under deviatoric stress of 25MPa, 20MPa and 15MPa, respectively, and the steady-state creep strain rate decreases with the decrease of deviatoric stress.

During the unloading stage, the relationship between deviatoric stress and steady-state creep strain rate can also be expressed by exponential function. The exponential function is used to fit and analyze the experimental data in the unloading stage. The fitting result is shown in Fig.12, the correlation coefficient reaches 0.997c, and the fitting function in the loading stage is simulated by the following equation.

$$\dot{\varepsilon} = 8.16 \times 10^{-4} \exp(0.328\sigma) \tag{6}$$

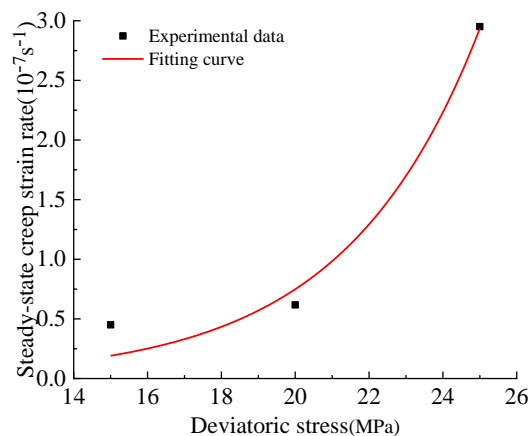


Fig.12: Fitting curve of steady-state creep strain rate and deviation stress at unloading stage

The steady-state creep strain rate of the three-stage creep test in the loading stage is higher than that in the unloading stage under the same deviator stress in the whole experiment. The creep deformation and steady-state creep strain rate in the loading stage increases as deviatoric stress increases, while the creep deformation in the unloading stage is very small, as shown in Fig. 7(a), and the steady-state creep strain rate decreases as deviatoric stress decreases, but the decrease is less than the increase in the loading stage. Creep of salt rock is mainly carried by dislocation motion in the crystal lattice [42]. Dislocation is a lattice defect with special structure carried by local relative slip between molecules. It will promote the occurrence and movement of dislocations when salt rock is in compression state. Strain hardening behavior of salt rock occur when the dislocation propagation is hindered [43]. The plastic behavior of salt rock carried by the continuous accumulation and sliding of dislocations. During the loading process of salt rock, the internal grain will produce the resistance stress and the external force to reach the balance because of the elastic stress of the crystal, the number of dislocations that increase gradually with the increase of external force, and the friction between crack walls of the new crack and the old crack generated in the plastic behavior of salt rock. In the unloading process, the resistance stress in the crystal doesn't disappear immediately, the elastic force is released when the dislocation moves in the opposite direction under its own elastic force. Stress resistance and decreases finally reach a steady-state with the increase of time, the dislocation moves back to its original position or beyond its original position as the loading continues, the dislocation repeats this reciprocating movement under cyclic loading.

The steady-state creep strain rate of the three-stage creep test in the loading stage is higher than that in the unloading stage under the same deviator stress, the reason is that the internal structure of the specimen will change to adapt to the corresponding stress state,

the number of dislocations in the specimen will increase, and the density will increase, so the internal movement of the specimen such as dislocation in place will produce a resistance to prevent further deformation when the specimen undergoes high deviatoric stress, so the specimen will produce a resistance to prevent further deformation during internal movements such as dislocations. Therefore, after the specimen undergoes high deviatoric stress in the loading stage, the resistance force will be generated inside the specimen to prevent the deformation during the unloading process, which leads to the steady-state creep strain rate decrease.

## 5. CONCLUSIONS

The creep characteristics of salt rock under loading and unloading conditions are studied. By using RC-2000 rock servo triaxial rheological testing machine of Wuhan Institute of Rock and Soil Mechanics, Chinese Academy of Sciences, the multi-stage loading and unloading creep tests of salt rock samples in Jintan, Jiangsu Province are carried out with constant confining pressure and the axial pressure increase. The conclusions are as follows:

(1) The results of SEM show that the crystal of pure salt rock is colorless. It can be seen from the microstructure that the surface of pure salt rock is extremely flat, smooth and dense, with no pores visible on the surface, indicating good tightness.

(2) The steady-state creep strain rate increases as the deviator stress increases in the whole test. During the loading stage, deviatoric stress has a great influence on the steady state creep strain rate, and the steady-state creep strain rate increases obviously when deviatoric stress increases, but during the unloading stage, although the steady-state creep strain rate decreases as the deviatoric stress decreases, the decrease range is small. The reason is that when the specimen undergoes high deviatoric stress, the resistance force will be generated inside the specimen to prevent the deformation.

(3) The Fractional Derivative model, Nishihara model, and Burgers model were used to fit and analyze the experimental data in the initial creep stage and the steady-state creep stage in the loading stage, the result is that the Fractional Derivative model is better. In the unloading stage, the deformation curve is almost a straight line, so the linear function is used to fit the creep curve, which shows that the unloading creep curve can be simulated by the linear function.

## 6. ACKNOWLEDGMENTS

The authors gratefully acknowledge the financial support provided by the National Natural Science Fund of China(No. 51834003, 51904039, 41702309), Postdoctoral Science Foundation Project Funded by State Key Laboratory of Coal Mine Disaster Dynamics

and Control (2011DA105287-BH201901), Chongqing Postdoctoral Innovation Program (CQBX201802), China Postdoctoral Science Foundation (2018M633318, 2019T120809), which are all greatly appreciated.

## 7. REFERENCES

- [1] Xie H., Liu J., Ju Y., Li J., and Xie L., Fractal Property of Spatial Distribution of Acoustic Emissions During the Failure Process of Bedded Rock Salt, *International Journal of Rock Mechanics and Mining Sciences*, Vol. 48, Issue 8, 2011, pp. 1344-1351.
- [2] Chen J., Jiang D., Ren S., and Yang C., Comparison of the Characteristics of Rock Salt Exposed to Loading and Unloading of Confining Pressures, *Acta Geotechnica*, Vol. 11, Issue 1, 2016, pp. 221-230.
- [3] Li Y., Liu W., Yang C., and Daemen J.J.K., Experimental Investigation of Mechanical Behavior of Bedded Rock Salt Containing Inclined Interlayer, *International Journal of Rock Mechanics and Mining Sciences*, Vol. 69, 2014, pp. 39-49.
- [4] Kang Y., Fan J., Jiang D., and Li Z., Influence of Geological and Environmental Factors on the Reconsolidation Behavior of Fine Granular Salt, *Natural Resources Research*, 2020.
- [5] Ma L., Wang M., Zhang N., Fan P., and Li J., A Variable-Parameter Creep Damage Model Incorporating the Effects of Loading Frequency for Rock Salt and its Application in a Bedded Storage Cavern, *Rock Mechanics and Rock Engineering*, Vol. 50, Issue 9, 2017, pp. 2495-2509.
- [6] He Y., Jiang D., Chen J., Liu R., Fan J., and Jiang, X., Non-Monotonic Relaxation and Memory Effect of Rock Salt, *Rock Mechanics and Rock Engineering*, Vol. 52, Issue 7, 2019, pp. 2471-2479.
- [7] Fan J., Xie H., Chen J., Jiang D., Liu C., Tiedeu, W.N., and Ambre J., Preliminary Feasibility Analysis of a Hybrid Pumped-Hydro Energy Storage System Using Abandoned Coal Mine Goafs, *Applied Energy*, Vol. 258, 2020.
- [8] Li J., Tang Y., Shi X., Xu W., and Yang C., Modeling the Construction of Energy Storage Salt Caverns in Bedded Salt, *Applied Energy*, Vol. 255, 2019.
- [9] Jiang D., Qiu H., Yi L., Ren S., Chen J., and Yang C., Similar Experimental Study of Cavity Building Using Large-Size Molded Salt Rock, *Chinese Journal of Rock Mechanics and Engineering*, Vol. 31, Issue 9, 2012, pp. 1746-1755.
- [10] Fan J., Liu W., Jiang D., Tiedeu W.N., and Daemen J.J.K., Time Interval Effect in Triaxial Discontinuous Cyclic Compression Tests and Simulations for the Residual Stress in Rock Salt. *Rock Mechanics and Rock Engineering*, Vol. 53, Issue 9, 2020, pp. 4061-4076.

- [11] Serata S. and Gloyna E.F., Reactor Fuel Waste Disposal Project Development of Design Principle for Disposal of Reactor Fuel Waste into Underground Salt Cavities, 1959.
- [12] Mills M.M., Stormont J.C., and Bauer S.J., Micromechanical Processes in Consolidated Granular Salt, *Engineering Geology*, Vol. 239, 2018, pp. 206-213.
- [13] Moghadam S.N., Mirzabozorg H., and Noorzad A., Modeling Time-Dependent Behavior of Gas Caverns in Rock Salt Considering Creep, Dilatancy and Failure, *Tunnelling and Underground Space Technology*, Vol. 33, 2013, pp. 171-185.
- [14] Liu W., Zhang Z., Fan J., Jiang D., and Daemen J.J.K., Research on the Stability and Treatments of Natural Gas Storage Caverns with Different Shapes in Bedded Salt Rocks, *IEEE Access*, Vol. 8, 2020, pp. 18995-19007.
- [15] Li J., Xu W., Zhang J., Li W., Shi X., and Yang C., Modeling the Mining of Energy Storage Salt Caverns Using a Structural Dynamic Mesh, *Energy*, Vol. 193, 2020, pp. 867-876.
- [16] Hunsche U. and Albrecht H., Results of True Triaxial Strength Tests on Rock Salt, *Engineering Fracture Mechanics*, Vol. 35, Issue 4-5, 1990, pp. 867-877.
- [17] Liu W., Zhang Z., Fan J., Jiang D., Li Z., and Chen J., Research on Gas Leakage and Collapse in the Cavern Roof of Underground Natural Gas Storage in Thinly Bedded Salt Rocks, *Journal of Energy Storage*, Vol. 31, Issue 10, 2020.
- [18] Senseny P.E., Hansen F.D., Russell J.E., Carter N.L., and Handin J.W., Mechanical Behaviour of Rock Salt: Phenomenology and Micromechanisms, *International Journal of Rock Mechanics and Mining Sciences* and, Vol. 29, Issue 4, 1992, pp. 363-378.
- [19] Liang W., Yang C., Zhao Y., Dusseault M.B., and Liu J., Experimental Investigation of Mechanical Properties of Bedded Salt Rock, *International Journal of Rock Mechanics and Mining Sciences*, Vol. 44, Issue 3, 2007, pp. 400-411.
- [20] Hansen F.D., Mellegard K.D., and Senseny P.E., Elasticity and Strength of Ten Natural Rock Salts, 1984, pp. 71-83.
- [21] Wang J., Zhang Q., Song Z., and Zhang Y., Creep Properties and Damage Constitutive Model of Salt Rock under Uniaxial Compression, *International Journal of Damage Mechanics*, Vol. 29, Issue 6, 2019, pp. 902-922.
- [22] Fuenkajorn K. and Phueakphum D., Effects of Cyclic Loading on Mechanical Properties of Maha Sarakham Salt, *Engineering Geology*, Vol. 112, Issue 1-4, 2010, pp. 43-52.
- [23] Zhao Y., Fan J., Jiang D., Jiang X., and Liu W., Experimental Study on the Dilatancy of Rock Salt From an Unloading Path, *International Journal of Geomate*, Vol. 17, Issue 63, 2019, pp. 224-232.
- [24] Ishizuka Y, Koyama H, and Komura S, Effect of Strain Rate on Strength and Frequency Dependence of Fatigue Failure of Rocks, *Proc International Symposium on Assessment and Prevention of Failure Phenomena in Rock Engineering*, Vol. 31, 2019, pp. 321-327.
- [25] Andargoli M.B.E., Shahriar K., Ramezanzadeh A., and Goshtasbi K., The Analysis of Dates Obtained from Long-Term Creep Tests to Determine Creep Coefficients of Rock Salt, *Bulletin of Engineering Geology and the Environment*, Vol. 78, Issue 3, 2019, pp. 1617-1629.
- [26] Carter N.L. and Hansen F.D., Creep of Rock Salt, *Tectonophysics*, Vol. 92, Issue 4, 1983, pp. 275-333.
- [27] Raj S.V. and Pharr G.M., Effect of Temperature on the Formation of Creep Substructure in Sodium-Chloride Single-Crystals, *Journal of the American Ceramic Society*, Vol. 75, Issue 2, 1992, pp. 347-352.
- [28] Mansouri H. and Ajalloeian R., Mechanical Behavior of Salt Rock under Uniaxial Compression and Creep Tests, *International Journal of Rock Mechanics and Mining Sciences*, Vol. 110, 2018, pp. 19-27.
- [29] Ran L., Zhang H., and Wang Z., Rock Long-Term Strength Parameters Determination of a Salt Cavern Gas Storage, *Advances in Civil and Industrial Engineering*, Vol. 353-356, 2013, pp. 1685-+.
- [30] Zhang H., Wang Z., Zheng Y., Duan P., and Ding S., Study on Tri-Axial Creep Experiment and Constitutive Relation of Different Rock Salt, *Safety Science*, Vol. 50, Issue 4, 2012, pp. 801-805.
- [31] Peng H., Fan J., Zhang X., Chen J., Li Z., Jiang D., and Liu C., Computed Tomography Analysis on Cyclic Fatigue and Damage Properties of Rock Salt under Gas Pressure, *International Journal of Fatigue*, Vol. 134, 2020.
- [32] He M., Li N., Zhu C., Chen Y., and Wu H., Experimental Investigation and Damage Modeling of Salt Rock Subjected to Fatigue Loading, *International Journal of Rock Mechanics and Mining Sciences*, Vol. 114, 2019, pp. 17-23.
- [33] Singh S.K., Fatigue and Strain-Hardening Behavior of Graywacke from the Flagstaff Formation, New-South-Wales, *Engineering Geology*, Vol. 26, Issue 2, 1989, pp. 171-179.
- [34] Fan J., Jiang D., Liu W., Wu F., Chen J., and Daemen J.J.K., Discontinuous Fatigue of Salt Rock with Low-Stress Intervals, *International Journal of Rock Mechanics and Mining Sciences*, Vol. 115, 2019, pp. 77-86.
- [35] Fan J., Chen J., Jiang D., Chemenda A., Chen J., and Ambre J., Discontinuous Cyclic Loading

- Tests of Salt with Acoustic Emission Monitoring, *International Journal of Fatigue*, Vol. 94, 2017, pp. 140-144.
- [36] Jiang D., Fan J., Chen J., Li L., and Cui Y., A Mechanism of Fatigue in Salt under Discontinuous Cycle Loading, *International Journal of Rock Mechanics and Mining Sciences*, Vol. 86, 2016, pp. 255-260.
- [37] Min H., Li W., and Luxia S., Experimental Study on the Creep Mechanical Properties of Carbonaceous Slate, *Electronic Journal of Geotechnical Engineering*, Vol. 19, 2014, pp. 4615-4630.
- [38] Chen J., Lu D., Wu F., Fan J., and Liu W., A Non-Linear Creep Constitutive Model for Salt Rock Based on Fractional Derivatives, *Thermal Science*, Vol. 23, 2019, pp. S773-S779.
- [39] Fan J., Chen J., Jiang D., Ren S., and Wu J., Fatigue Properties of Rock Salt Subjected to Interval Cyclic Pressure, *International Journal of Fatigue*, Vol. 90, Issue 9, 2016, pp. 109-115.
- [40] Wang J., Liu X., Song Z., and Shao Z., An Improved Maxwell Creep Model for Salt Rock, *Geomechanics and Engineering*, Vol. 9, Issue 4, 2015, pp. 499-511.
- [41] Fan J., Liu P., Li J., and Jiang D., A Coupled Methane/Air Flow Model for Coal Gas Drainage: Model Development and Finite-Difference Solution, *Process Safety and Environmental Protection*, Vol. 141, Issue 8, 2020, pp. 288-304.
- [42] Schoenherr J., Schleder Z., Urai J.L., Littke R., and Kukla P.A., Deformation Mechanisms of Deeply Buried and Surface-Piercing Late Pre-Cambrian to Early Cambrian Ara Salt from Interior Oman, *International Journal of Earth Sciences*, Vol. 99, Issue 5, 2010, pp. 1007-1025.
- [43] Chen J., Peng H., Fan J., Zhang X., Liu W., and Jiang D., Microscopic Investigations on the Healing and Softening of Damaged Salt by Uniaxial Deformation from CT, SEM and NMR: Effect of Fluids (Brine and Oil), *Rsc Advances*, Vol. 10, Issue 5, 2020, pp. 2877-2886.

---

Copyright © Int. J. of GEOMATE. All rights reserved, including the making of copies unless permission is obtained from the copyright proprietors.

---